PHILOSOPHICAL TRANSACTIONS OF THE ROYAL SOCIETY A MATHEMATICAL, PHYSICAL & ENGINEERING SCIENCES

Metastable Pitting Corrosion of Stainless Steel and the Transition to Stability

P. C. Pistorius and G. T. Burstein

Phil. Trans. R. Soc. Lond. A 1992 **341**, 531-559
doi: 10.1098/rsta.1992.0114

Metastable pitting corrosion of stainless steel and the transition to stability

By P. C. Pistorius† and G. T. Burstein

Department of Materials Science and Metallurgy, University of Cambridge, Pembroke Street, Cambridge CB2 3QZ, U.K.

Contents

The evolution of corrosion pits on stainless steel immersed in chloride solution occurs in three distinct stages: nucleation, metastable growth and stable growth. This paper describes the growth of metastable corrosion pits on stainless steel immersed in chloride solution, and their transition to stability. The rate of growth of individual corrosion pits is controlled by diffusion of the dissolving metal cations from the pit interior, the surface of which is saturated with the metal chloride. This process is independent of electrode potential. Analysis of the diffusion yields a critical value of the product of the pit radius and its dissolution current density (termed the 'pit stability product') below which the pit is metastable and may repassivate, and above which the pit is stable. The critical value of the pit stability product for stainless steel in chloride solution is 0.3 A m^{-1}. All pits, whether metastable, or destined to become stable, grow initially in the metastable condition, with a pit stability product which increases linearly with time, but below the critical value. Metastable growth requires a perforated cover over the pit mouth to provide an additional barrier to diffusion,

† Present address: Department of Materials Science and Metallurgical Engineering, University of Pretoria, Pretoria 0002, South Africa.

Phil. Trans. R. Soc. Lond. A (1992) **341**, 531–559
Printed in Great Britain

enabling the aggressive pit anolyte to be maintained. In this state pits grow at a constant mean current density which is maintained by periodic partial rupture of the cover. Stable pit growth is then achieved when the cover is no longer required for continued propagation, and the pit depth is itself a sufficient diffusion barrier; stability is characterized by a constant mean pit stability product above the critical value. If the cover is lost prematurely, before the critical pit stability product is achieved, the pit anolyte is diluted and repassivation is inevitable.

In contrast to the growth rate of individual pits, the distribution of pitting current transients is dependent on electrode potential: the pit nucleation site, particularly its geometry, is exclusively responsible for this potential distribution. It is proposed that shallower, more-open sites are activated only at higher potential and higher current density, and are consequently more likely to achieve stability.

1. Introduction

Most metals which exhibit low corrosion rates in aqueous environments owe their corrosion resistance to a thin passivating oxide film which covers the metal surface. Pitting corrosion arises where passivity is lost at localized points on the metal surface, usually under the action of aggressive anions; chloride is the most commonly encountered aggressive anion causing pitting corrosion in many metals and alloys. Corrosion pits are holes developed on the metal surface, which propagate very rapidly by anodic dissolution of the metal, the supporting cathodic reaction occurring on the surrounding passive surface: stable pits are formed only if the electrode potential is more positive than the pitting potential (Szklarska-Smialowska 1986).

Once a pit has started growing, its growth is sustained by the development of a highly aggressive anolyte inside the pit (Evans 1951; Galvele 1976). The anolyte has a low pH as a result of hydrolysis of the dissolving metal cations. The anolyte also carries an enhanced concentration of anions, because these migrate into the pit to maintain anolytic charge neutrality. Because of the development of the aggressive anolyte, pit growth is self-sustaining. Since pits tend to continue growing once they have become established, the susceptibility of a metal to pitting corrosion must be linked to the ease with which stable pits can be formed in the first place: very many pits which nucleate do not propagate indefinitely, but repassivate after a very short period of growth.

For stainless steels in chloride solutions, the formation of a stable pit is preceded by electrochemical noise. The noise events take the form of fluctuations of the electrode potential in open circuit or under galvanostatically applied currents, or current fluctuations if the metal is held under potential control (Williams *et al.* 1985; Frankel *et al.* 1987). Each noise event results from the nucleation, growth and repassivation of a microscopic corrosion pit. Pits which cease growing and repassivate in this way are described as metastable (Stockert 1988). Metastable pits in themselves cause no great damage to the metal in many service conditions, since the final diameter of such pits is only of the order of a few micrometres. Their importance lies in the information that they can impart about the formation of stably growing pits; such information is expected since there appear to be 'no discernible differences' between metastable pit growth and the initial growth of stable, destructive pits (Isaacs 1989).

PHILOSOPHICAL TRANSACTIONS OF THE ROYAL SOCIETY A MATHEMATICAL, PHYSICAL & ENGINEERING SCIENCES

This paper describes the development of metastable pits on stainless steel surfaces in chloride solution, and their transition to stability.

2. Experimental techniques

The experimental approach was an examination of the nature of the train of current transients that emanate from passive stainless steel held under potential control in chloride solution. Because the current transients can be small in magnitude, it is necessary to restrict the exposed surface area of the specimen tested so as to minimize the passive current flowing from the electrode as a whole; this also reduces the frequency of events, allowing sufficient separation to examine individual transients. By using a circular surface microelectrode of diameter 50 μm the passive current was reduced to less than 0.5 nA (this was the background noise level in the electronic circuits), allowing observation of pitting currents down to that level.

The stainless steel examined was American Iron and Steel Institute (AISI) type 304, supplied by Goodfellow Materials (The Science Park, Cambridge CB4 4DJ, U.K.) in the form of annealed wire of diameter 50 μm. The steel was analysed by energy-dispersive X-ray analysis (EDX) using a Link EDX system coupled to a Camscan S4 scanning electron microscope (SEM). Such analysis gave (in weight percent): Cr 17.9, Ni 10.4, Mn 0.8, Si 0.4, Fe balance. No sulphur was detected. The carbon content was not analysed: the specification of AISI type 304 allows a maximum carbon content of 0.08%. No sulphide inclusions could be detected by either optical microscopy or SEM/EDX: this places an upper limit of *ca.* 1 μm on the size of any sulphides which may be present in the alloy. The material was not sensitized as tested by electrolytic etching for 90 s at 10 kA m^{-2} in 10% oxalic acid (American Society for Testing of Metals 1989).

Robust electrodes were manufactured by casting a support of epoxy resin around the wire. The exposed circular end of the wire served as the test surface. Just before the start of electrochemical testing, the electrode was wet-ground to a 1200 grit finish by using silicon carbide paper. It was transferred to the cell within one minute after grinding. Electrochemical testing commenced after a further 40 s during which the electrode was left in open circuit.

The stainless steel microelectrode was tested in a conventional three-electrode cell of capacity 100 cm^3. A saturated calomel reference electrode (SCE) (against which all potentials in this paper are presented) was connected to the cell through a Luggin probe, the capillary tip of which was opposite the end of the working electrode, *ca.* 5 mm away. A cylindrical platinum counter electrode, of diameter and height 15 mm surrounded the ends of the working electrode and the Luggin probe. The potential of the working electrode was controlled with a battery-powered potentiostat (built in our laboratory). A Faraday cage screened the potentiostat and the cell from extraneous interference. A Keithley 428 current amplifier converted the current supplied by the potentiostat to a voltage signal. The output from the current amplifier was recorded on a digital transient recorder (Datalab 1080 or CIL 1580).

The electrolyte contained 0.8 M NaCl and 0.2 M HCl, prepared from analytical grade reagents and double-distilled water. Its pH was 0.7 and its conductivity 13 S m^{-1}. The contents of the cell were deaerated by purging with deoxygenated high-purity nitrogen for at least an hour before, and during experiments.

Experiments were performed at ambient temperature (290 ± 3 K) by sweeping the potential positively from −0.45 V_{SCE} (just below the open-circuit corrosion potential)

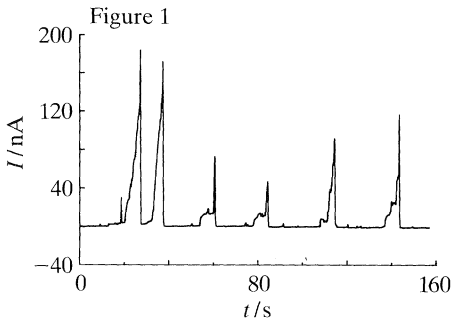

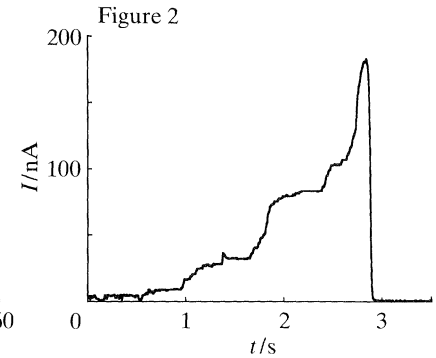

Figure 1. Train of current transients from metastable pit growth. 50 μm electrode of type 304 stainless steel held at 0.1 V in a solution of 1 M Cl^-, pH 0.7.

Figure 2. Single current transient from a metastable pit, showing the typical way in which the current rises in a series of steps. Repassivation is preceded by a sharp current increase. Electrode potential 0.3 V.

at a rate of 2 mV s^{-1}. Some experiments involved sweeping the potential from the same lower limit at the same rate to a defined holding potential to observe transients at constant potential.

3. Current transients from metastable pit growth

Current transients from metastable pit growth were observed at potentials greater than about −0.19 V in the acidic 1 M Cl^- solution. None was observed in chloride-free sulphate solutions. However, it must be borne in mind that only transients of 0.5 nA peak current or larger could be observed above the background noise; recent experiments of Riley *et al.* (1991) indicate the existence of smaller transients, in the range of tens of pA, ascribed to pit nucleation events. The peak currents of the transients observed in this work showed a general tendency to increase with increased potential, and varied from less than 1 nA to more than 10 μA. At constant potential, a similar train of events is observed as shown in figure 1. Each transient displays the well-documented typical shape for stainless steel of a slow rise in current followed by a rapid fall (Forchhammer & Engell 1969; Stockert 1988). The transients in figure 1 show a further feature that has not been reported elsewhere: the increase of the current from each metastable pit is not smooth. Rather, the current (I) rises in a number of rapid increments, separated by regions where the current remains approximately constant. This is illustrated in figure 2, a detail of one transient. The transients of figures 1 and 2 also show that the final repassivation event, observed as a fast current decay, is immediately preceded by a rapid increase in current. This final current jump before repassivation is common to all transients. The initial propagation of stable pits also follows the pattern of stepwise rises in current, with the difference that none of these fast rises leads to repassivation.

Electron-microscopic examination of the surface after pitting experiments revealed the presence of microscopic pits. The pits ranged in diameter from *ca.* 100 nm to more than 10 μm. The mouths of all pits, down to the smallest size observed, were approximately circular. Where the pit interiors could be examined (larger pits of *ca.* 10 μm diameter), they were smooth.

Integration of the current-time record from each metastable pit gives the anodic charge which passed during pit growth. This anodic charge was compared with the

PHILOSOPHICAL TRANSACTIONS OF THE ROYAL SOCIETY A MATHEMATICAL, PHYSICAL & ENGINEERING SCIENCES

Figure 3

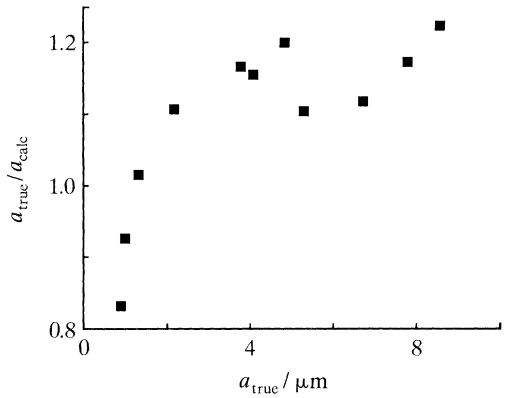

Figure 4

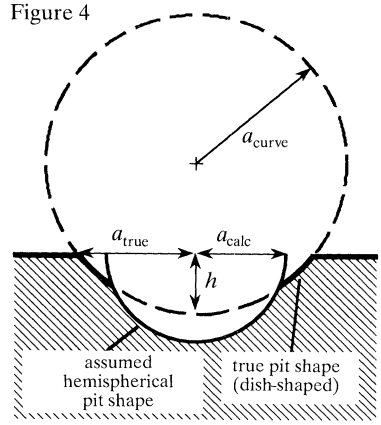

Figure 3. Comparison between the measured radii of metastable pits (a_{true}) and the radii calculated from the anodic charges on the assumption that the pits are hemispherical (a_{calc}).

Figure 4. The relationship between the true shape of pits (dish-shaped), and the size of a hemispherical pit which has the same volume. The true radius of the mouth of the dish-shaped pit (a_{true}) is larger than the radius of the hemisphere (a_{calc}); this radius is in turn larger than the true depth of the pit (h). The true pit shape is assumed to be a spherical section, where the radius of curvature is a_{curve}. After Alkire & Wong (1988).

measured size of microscopically observed pits. The aim of this comparison was to determine whether the pits were hemispherical. The knowledge is important to enable the surface area of the growing pit to be determined from the charge passed, and thence the current density (i). The expected radius of each pit was calculated from the anodic charge by using Faraday's law on the assumptions that the pit was hemispherical, and that the metallic components of the alloy are oxidized to Fe^{2+}, Cr^{3+}, and Ni^{2+} during dissolution. For an alloy of composition given above, and of density 7.92 Mg m^{-3} (Brandes 1983), the calculated average oxidation state of the cations produced by dissolution is 2.19, and the volume of metal dissolved per unit anodic charge, $k_v = 3.31 \times 10^{-11}$ m^3 C^{-1}.

The average radius of each pit was determined from SEM photography by measuring the area of the pit mouth with a planimeter, taking into account the tilt angle in the microscope. The radii thus measured, a_{true} are compared with the calculated pit radii, a_{calc} in figure 3. The diagram shows that the pit mouths are mostly slightly larger than calculated, especially for larger pits. That this discrepancy could arise from incorrect assumption of the dissolved cation oxidation states is thought to be unlikely, since these oxidation states correlate well with those measured from artificial pits of this steel (Hunkeler & Böhni 1987). In addition, the mouths of the smallest pits measured are actually smaller than calculated (see figure 3): if the dissolved volume were really greater than that calculated from the anodic charge, the effect is expected to be the same for all pit sizes.

A more likely explanation for the discrepancy between the calculated and true pit radii is that the larger pits are slightly dish-shaped, with a depth smaller than the radius of the pit mouth, similar to the shape reported by Alkire & Wong (1988). If the pit is not hemispherical, then its true internal surface area is larger than the value calculated on the assumption of a hemispherical shape, and thus current density

Figure 5

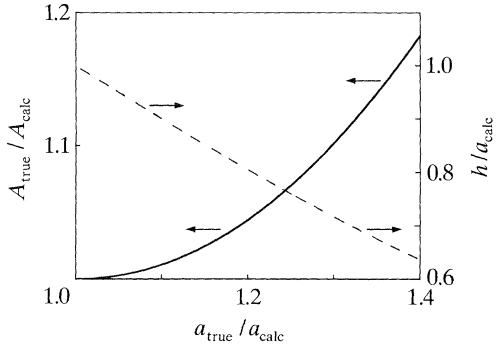

Figure 6

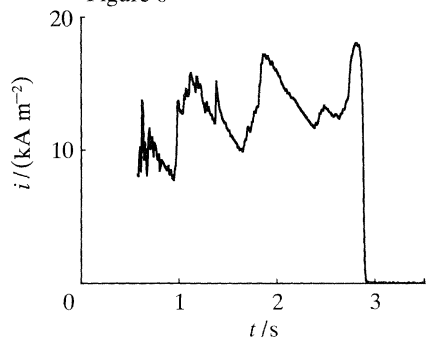

Figure 5. The ratios of the true pit depth to the calculated value (broken line), and the true pit surface area to the calculated value (solid line), for pits which are increasingly dish-shaped.

Figure 6. Calculated current density in the metastably growing pit of figure 2. Before repassivation at 2.9 s the current density fluctuates around a mean value which is approximately constant with time.

calculations are erroneously large. Figure 4 illustrates the geometrical relationship between the calculated size of the assumed hemispherical shape and the actual shape of the pit. The true radius of the pit mouth (a_{true}) is larger than the calculated radius (a_{calc}) and the true pit depth (h) is smaller than the calculated depth. The volume (V) and the area (A) of the dish-shaped pit are respectively (Alkire & Wong 1988):

$$V = \tfrac{1}{3}\pi h^2(3a_{\mathrm{curve}} - h), \tag{3.1}$$

$$A = 2\pi a_{\mathrm{curve}}\, h, \tag{3.2}$$

where a_{curve} is the radius of the sphere of which the pit forms a section.

Equations (3.1) and (3.2) were used to quantify the relationships between the depth and area of the hemispherical pits, and those of dish-shaped pits, for pits of equal volume. The results are shown in figure 5, where the ratio of the true and calculated pit depths, and the ratio of the true and calculated pit surface areas (A_{true} and A_{calc}) are expressed as a function of the degree to which the pit shape deviates from hemispherical (expressed as $a_{\mathrm{true}}/a_{\mathrm{calc}}$). The figure illustrates that the difference between the true and calculated areas is not very large. The largest value of $a_{\mathrm{true}}/a_{\mathrm{calc}}$ which was observed, was 1.22 (see figure 3), and figure 5 shows that the corresponding true pit area is then only 5% larger than the value calculated from the anodic charge. It is thus justified to assume that the pits are hemispherical for calculation of the current density, and this assumption was made for the current density data presented below.

The calculated current density flowing from the metastably growing pit of figure 2 is shown in figure 6. The pit current density fluctuates around a mean value of some 12 kA $\mathrm{m^{-2}}$; this mean value does not change significantly with time until the onset of repassivation at 2.9 s. The regions of constant current in figure 2 are reflected as decaying current density in figure 6, but the current density increases sharply where the current increases sharply. The high average current density is equivalent to a radial penetration rate of 1.4 mm $\mathrm{h^{-1}}$, which emphasizes the highly destructive nature of pitting corrosion. For each metastable pit examined the current density was observed to be nearly independent of time, consistent with the work of others (Frankel *et al.* 1987; Stockert 1988); this implies that the absolute current in each transient increases approximately with the square of time.

PHILOSOPHICAL TRANSACTIONS OF THE ROYAL SOCIETY A MATHEMATICAL, PHYSICAL & ENGINEERING SCIENCES

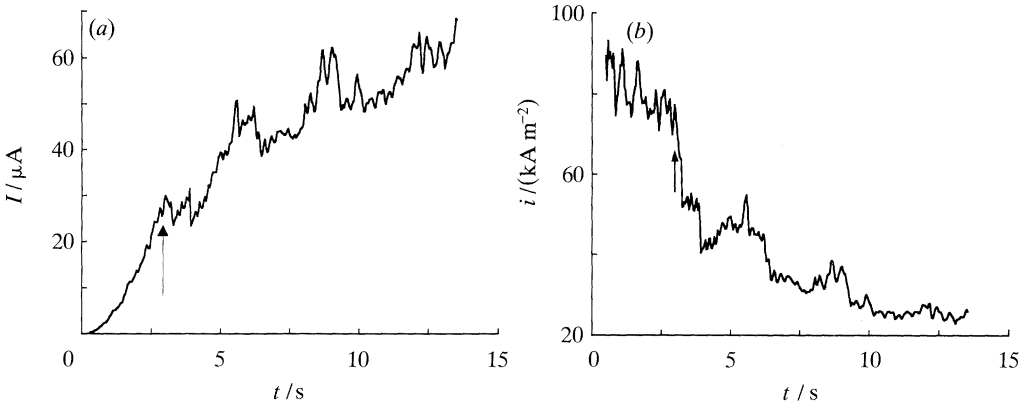

Figure 7. Early stages of the growth of a stable pit at 0.56 V. (*a*) Current transient, which indicates that the current initially increases with an increasing slope, but rises more slowly after an inflexion point is reached; the current is more noisy after the inflexion point. (*b*) The calculated current density in the stable pit is initially approximately constant, but decreases after the current has reached the inflexion point. The inflexion point in the current is marked with an arrow in both diagrams.

Although the average current density in each metastably growing pit is approximately constant with time, the average current density in *different* pits observed at the same potential was found to vary by a factor of more than five (see §6*c*).

4. Current transients from stable pit growth

Current transients from stable pits showed an initial form similar to that of metastable pits. Figure 7*a* illustrates this: the current rises approximately in proportion to t^2, but only up to $t = 3$ s. The feature is also well demonstrated in figure 7*b*, where for the same stable pit the average current density is approximately constant for the first 3 s, with a mean value of *ca.* 80 kA m^{-2}. The same sharp rises in the current density (corresponding to sharp rises in current) are observed in this region, in a similar fashion to the behaviour of metastable pits (cf. figures 2 and 6). Beyond 3 s, which constitutes an inflexion point in figure 7*a*, the overall rate of rise of the current with time ($\mathrm{d}I/\mathrm{d}t$) decreases with time. The inflexion point in the current is indicated in both figures. (Because of the noise on the current transient, it contains many inflexion points. However, there is only one point on the transient where the slope $\mathrm{d}I/\mathrm{d}t$ shows a permanent change from an increase, on average, to an overall decrease with time: this is the inflexion point considered here.) The same transition from growth at constant i ($I \propto t^2$) to a current density that decreases with the square root of time ($I \propto \sqrt{t}$) was reported by Frankel *et al.* (1987). The noise on the current in figure 7*a* precludes a clear decision on whether the current and current density follow $\sqrt{t}$ relationships, but it is clear that the indicated inflexion point marks the start of a permanent change in the pit growth rate. (It is shown below (§5) that the two regions of figure 7*b* can be described by the product ia, where a is the pit radius.)

The noise on the current for times greater than 3 s is reminiscent of fluctuations in the current flowing from artificial pits on type 304 stainless steel growing under diffusion control in chloride solution (Ezuber *et al.* 1989) and for iron electrodes dissolving at high current density in concentrated chloride solutions (Li *et al.* 1990).

In both cases, the metal dissolves through a salt film: Li *et al.* described the current fluctuations as a dynamic competition between the rate at which the salt film forms and the rate at which it dissolves.

Figure 7 emphasizes the point made elsewhere (Isaacs 1989) that the *initial* growth of stable pits appears to be indistinguishable from that of metastable pit growth, at least kinetically. In both cases the current density is approximately constant with time. The clear implication is that all pits grow initially metastably. The difference between metastable and stable pit growth is that the former is terminated by repassivation, while stable pits continue to grow and eventually show a transition in the growth rate. The transition is characterized by a permanent change from growth at constant current density to a current density that decreases with time. Moreover, it is this transition in growth rate which marks the transition from metastability to stability, as described in a theoretical criterion developed in §5.

5. A criterion for stable pit growth

(*a*) *Theoretical considerations for stable pit growth*

The aggressive anolyte developed within a propagating pit results from a low pH and a high chloride concentration (§1). The concentration of metal cations within the anolyte is a useful measure of the aggressiveness, since it is this concentration which produces the change in electrolyte composition. Others (Gaudet *et al.* 1986; Hakkarainen 1990) have shown that for type 304 stainless steel, the metal cation concentration in solution must be greater than *ca.* 75–80% of saturation of the chloride salt to prevent repassivation: the saturation concentration is *ca.* 4 M. If the metal cation concentration is less than *ca.* 75% of saturation (i.e. below 3 M), the anolyte is not aggressive enough to sustain rapid dissolution of the alloy, and repassivation is inevitable.

The metal cation concentration on the surface of a growing pit is determined by the balance between the production of cations by dissolution of the metal, and transport of cations away from the dissolving surface. The contributions of convection and migration are neglected in this analysis. It is justified to neglect convection since the pits considered here (diameter less than about 10 μm) are far smaller than the steady state thickness of the diffusion boundary layer (*ca.* 100 μm; Vetter 1967). The effect of migration can also justifiably be neglected since it is counteracted approximately by a decrease in the diffusion coefficient in the concentrated pit solution (Hunkeler & Böhni 1987; Gaudet *et al.* 1986; Alkire & Wong 1988).

A final simplifying assumption is that diffusion is in a steady state. This assumption can be made because the growth period of metastable pits is of the order of seconds, much larger than the time required to establish a diffusional steady state. The time constant associated with the establishment of a diffusional steady state is of the order of a^2/D, where D is the diffusion coefficient (*ca.* 10^{-9} m^2 s^{-1} for ions in aqueous solution). Thus for a pit of radius $a = 1$ μm, it takes *ca.* 1 ms to establish a steady state.

It is established in Appendix A that the steady-state diffusion rate ($\partial m/\partial t$) from an open hemispherical pit is given by

$$\partial m/\partial t = 3aD\Delta C, \tag{5.1}$$

where m is the quantity (in mol) of cations, D is the diffusion coefficient of metal

cations in solution, and ΔC is the concentration difference between the interior surface of the pit and the bulk solution far away from the pit. Rearranging equation (5.1), with $\partial m/\partial t = I/zF$ and $I = 2\pi a^2 i$ for a hemispherical pit gives the degree of concentration at the surface of the pit as

$$\Delta C = (2\pi/3zFD)\, ia, \tag{5.2}$$

where z is the average oxidation state of the cations (2.19), and F is the Faraday constant. An implicit assumption in equation (5.2) is that the entire anodic dissolution current is carried by the diffusion of metal cations out of the pit. In fact, some cations are not transported out of the pit, but are retained in the volume created by dissolution. However, the cations accumulated in this manner are but a small fraction of the total amount dissolved, even if the pit anolyte is concentrated in metal cations; the fraction is less than 3 % if the pit anolyte is saturated with the metal salt.

If the metal cation concentration in the bulk solution is zero, ΔC is the surface concentration, and this must be greater than 3 M to sustain pit growth. Equation (5.2) thus shows that sustenance of pit growth requires a minimum product of the current density (i) and the pit depth, or radius (a). This is akin to the argument put forward by Galvele (1976, 1981), that the requirement for pit stability for a one dimensional pit of depth x is that the product ix must exceed a certain critical value.

Using $\Delta C = 3$ M, $z = 2.19$, $F = 96485$ C mol^{-1} and $D = 10^{-9}$ m^2 s^{-1}, the critical value of ia is calculated to be 0.3 A m^{-1}. The diffusion analysis defines a narrow range of ia over which pits are stable. The lower limit is set as above, with the requirement that ΔC must exceed 3 M; the upper limit is defined by the solubility of the metal salt. Experiments with artificial pits have indicated that the pit anolyte can become supersaturated by a factor of *ca.* 1.5 before the salt precipitates (Hunkeler & Böhni 1987). This provides the upper limit on ia. Taking the saturation concentration of the metal salt to be 4 M (Kuo & Landolt 1975), the requirement for stable pit growth of an open pit is summarized as

$$0.3 \text{ A m}^{-1} \leqslant ia \leqslant 0.6 \text{ A m}^{-1}. \tag{5.3}$$

The product ia is called the 'pit stability product' for the rest of this paper.

The minimum pit stability product described above is in close agreement with Frankel *et al.* (1987), who showed that pits growing on type 302 stainless steel in chloride solution at constant current density become stable only if the factor $i\sqrt{t}$ exceeds a critical value of 107 kA s$^{\frac{1}{2}}$ m^{-2}, where t is the time for which the pit has been growing at constant current density. The close agreement is shown as follows. For a hemispherical pit growing at constant current density from time zero the radius is proportional to the product of the current density and time:

$$a = k_{\mathrm{v}}\, it, \tag{5.4}$$

where $k_{\mathrm{v}} = 3.31 \times 10^{-11}$ m^3 C^{-1} (see §3). It is apparent that the product $i\sqrt{t}$ can be expressed as

$$i\sqrt{t} = \sqrt{(ia/k_{\mathrm{v}})}. \tag{5.5}$$

Substituting $ia = 0.3$ A m^{-1} yields $i\sqrt{t} = 95$ kA s$^{\frac{1}{2}}$ m^{-2}, very close to the experimental value described above.

(*b*) *Application of the pit stability criterion to experimental results*

The evolution of the pit stability product for the transient shown in figure 2 is displayed in figure 8. Throughout the life of this metastable pit, the pit stability

Figure 8

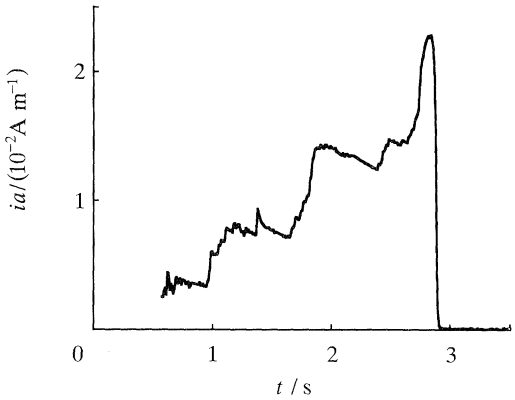

Figure 9

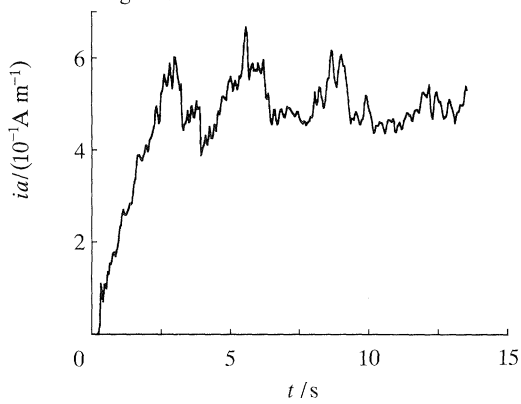

Figure 8. Development of the product of pit depth and current density (the pit stability product) during metastable pit growth. The pit stability product is smaller than 0.3 A m^{-1} – the minimum required for stable growth of an open pit – throughout. Calculated from the current transient in figure 2.

Figure 9. Development of the pit stability product (ia) for a pit which grew to become stable. The pit stability product is initially smaller than 0.3 A m^{-1} in a pit which grows to be stable. This period of metastable growth is followed by one during which ia fluctuates around a nearly constant value within the allowable band for stable growth (0.3–0.6 A m^{-1}). Data of figure 8.

product remains far below the minimum criterion defined by equation (5.3). It was indeed found in the present analysis of more than 200 metastable pits, that in no case did ia ever exceed 0.3 A m^{-1}.

In the case of stable pits, ia is initially also smaller than the required minimum value of 0.3 A m^{-1}, as shown in figure 9 as a function of time for the stable pit shown in figure 7. It is apparent from figure 9 that the pit stability product is originally far smaller than the minimum for stability. Figure 9 reveals two regions of pit growth in line with figure 7. In the first, the pit stability product increases approximately linearly with time (indicating that the current density is constant, equation (5.5)). Then, at a time which coincides with the inflexion point of figure 7*a* (3 s), the pit stability product levels off and does not increase further. Instead, it fluctuates noisily around a mean value which is approximately constant. The first region of stable pit growth is thus kinetically identical to the growth of metastable pits, with a constant current density. During the second period, which is only observed for stable pits, the pit grows with a constant average pit stability product. It is also worth noting that for a hemispherical pit which grows at a constant value of ia from $t = 0$, the current density is inversely proportional to $\sqrt{t}$ (see figure 7*b* for $t > 3$ s): this follows from the proportionality of the radial pit growth rate to the current density.

The average ia value during the second period, where the pit is stable, is 0.5 A m^{-1} from figure 9, which is in the allowable band defined by equation (5.3). For six stable pits whose current transients were recorded for times long enough to allow the calculation of the average ia value, the average was found to be 0.48 ± 0.03 A m^{-1} (95% confidence interval), also within the band defined by equation (5.3). Thus the second period of pit growth, in which it becomes stable, is adequately described by the pit stability criterion.

However, the question remains how metastable pits grow for several seconds before repassivating, even though pit growth is apparently precluded by an insufficiently large pit stability product; the same question is raised about the early

PHILOSOPHICAL TRANSACTIONS OF THE ROYAL SOCIETY A MATHEMATICAL, PHYSICAL & ENGINEERING SCIENCES

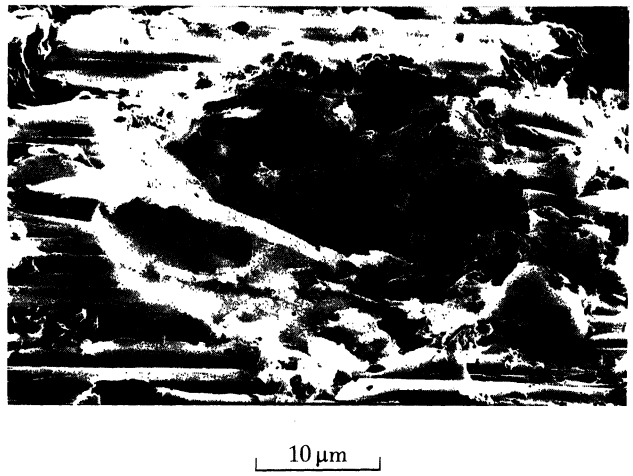

Figure 10. Photomicrograph of a corrosion pit showing remnants of the cover over the pit mouth. The ligaments which extend into the pit interior are clearly part of what had been the original metal surface.

stage of stable pit growth, during which *ia* is below the stability band. If $ia < 0.3$ A m^{-1}, the depth of the pit alone is an insufficient barrier to diffusion to sustain the required metal cation concentration at the dissolving pit surface. The pit cannot propagate: it must repassivate because the anolyte is not aggressive enough. All pits, whether they grow to become stable, or whether they die at the metastable stage, proceed initially with a pit stability product less than the critical 0.3 A m^{-1}. The implication is that there is, at least initially, an additional barrier to diffusion, in addition to the pit depth. This additional barrier is provided by a flawed cover, as described below.

(*c*) *The growth of covered pits*

The presence of covers over pits growing on type 304 stainless steel in chloride solution has been observed earlier (Schwenk 1964; Rosenfeld & Danilov 1967; Isaacs & Kissel 1972; Isaacs 1974; Mankowski & Szklarska-Smialowska 1975, 1977), although the pits were larger than the ones considered here. Isaacs (1974) found that mechanical disruption of the cover led to repassivation of the pit, clearly demonstrating its importance for sustained pit growth. Also clear is that any cover over a propagating pit must contain a flaw (such as a hole) for ionic current to pass between the pit anolyte and the exterior electrolyte. Although no clear cover was observed microscopically for the very small pits examined in the present work, some remnants of what had probably been a cover are seen in the micrograph presented in figure 10. Ligaments of solid material are observed to protrude from the edge of the pit into the middle: these ligaments are clearly part of the original metal surface. The cover consists of the passive film which had originally covered the unattacked metal, and probably also contains a vestige of unreacted metal.

The first question is why many of the covered pits are metastable: in many cases the pits repassivate. If the pit cover is the major diffusion barrier, repassivation implies that the pit cover is lost somehow. When the pit cover is lost, the pit anolyte dilutes and dissolution is no longer possible. One way that the pit cover may be lost is through mechanical rupturing caused by the osmotic pressure difference across the

PHILOSOPHICAL TRANSACTIONS OF THE ROYAL SOCIETY A MATHEMATICAL, PHYSICAL & ENGINEERING SCIENCES

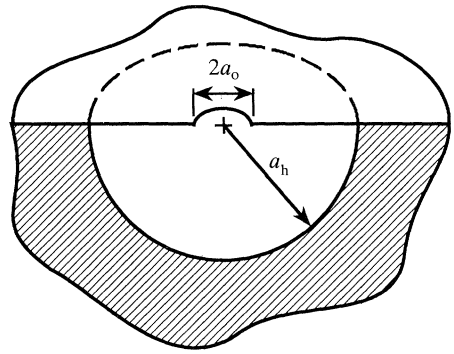

Figure 11. Assumed configuration of a covered hemispherical pit (shown in section). The pit, with radius a_h, is covered by a film which contains a circular hole of radius a_o. The hole is concentric with the hemisphere.

cover, which is generated by the concentration difference between the pit anolyte and the electrolyte outside the pit (Mankowski & Szklarska-Smialowska 1975, 1977).

Such rupture events are proposed to be the origin of the sharp current increases seen in metastable pit growth transients (see figures 1 and 2) as well as in the early growth transients of stable pits. Each rapid current increment reflects partial rupture of the cover, increasing the size of the perforation in the cover, or opening up new holes. The larger or more numerous holes allow more rapid diffusion of cations from the pit interior, which gives the larger current. The final sharp increase in current seen in transients from metastable pits immediately prior to repassivation (see figures 2 and 3), also arises from rupture of the cover: in this case the rupture causes dilution of the pit anolyte to such an extent that the pit repassivates, even though the more rapid transport of metal cations through the enlarged hole causes a transient increase in current. According to this rationale, pit growth at a constant average current density in the metastable régime requires a cover over the mouth of the pit, but it also requires the size and/or the number of holes in the cover to increase with time. This introduces a probabilistic element into the pit growth process: pit survival with each rupture hinges on whether rupture of the cover accelerates mass transport to the extent that the pit repassivates, or whether it only leads to more rapid growth (higher current). Because the attainment of a stable pit then depends on the mechanical properties of the cover, random variation in these properties over the metal surface contributes to the stochastic nature of pitting corrosion.

Once the pit stability product (ia) achieves a value in the stability band defined by equation (5.3), the pit can continue to grow without a cover over its mouth: it has attained stability. Until it reaches the stability band, its continuing propagation requires the pit cover to maintain the aggressive ion concentration. Thus the passive film plays an apparently paradoxical role during the early stages of pit growth. Whereas it normally provides the excellent corrosion resistance of the passive metal, it actually aids the early growth of corrosion pits, by forming a cover over the mouth. This contention is supported by the observation that the nature of the passive film has a strong effect on pit stability (Isaacs & Kissel 1972).

It is of significance to consider the expected size of the hole in the pit cover. The simplest configuration is that shown in figure 11: the pit cover is assumed to contain a circular hole (radius a_o), which is concentric with the hemispherical pit (radius a_h).

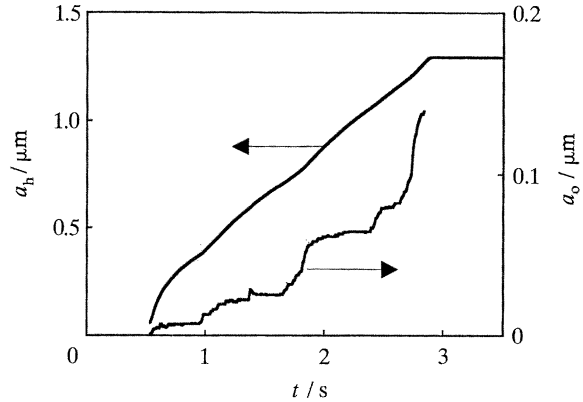

Figure 12. Calculated radius of the opening in the cover over the pit, compared with the pit radius. The figure illustrates metastable growth (data of figure 2), during which a cover is present over the mouth of the pit. The hole in this cover is much smaller than the pit radius.

This configuration is considered because its simplicity facilitates mathematical analysis, and because there is no evidence to indicate that it may be incorrect, although other configurations such as cracks or multiple holes are possible. However, because the observed pits are hemispherical, centrosymmetry is implicit, and Stockert (1988) has shown some evidence that the simple configuration may be correct. The diffusion rate from the interior of a covered pit is given by

$$\partial m/\partial t = SD\Delta C, \tag{5.6}$$

where S is the 'shape factor' (Holman 1986; see Appendix A). The shape factor has the unit of length and quantifies the effect of geometry on diffusion. The relevant shape factor is given by

$$S = 2a_o/(1-a_o/\pi a_h). \tag{5.7}$$

This shape factor is estimated in Appendix A, where some experimental confirmation of the derived expression is also presented. It should be noted that equation (5.7) applies only if the thickness of the cover is much smaller than the size of the hole in the cover. Equation (5.7) indicates that the shape factor approaches $2a_o$ if $a_o \ll a_h$. If $a_o = a_h$ (i.e. an open pit with no cover), the shape factor is then approximately $3a_o$, consistent with equation (5.1).

Thus the current from a covered hemispherical pit is given by

$$I = ca_o zFD\Delta C, \tag{5.8}$$

where c is a dimensionless constant with a value between 2 and 3. Using the same parameters as defined above, the size of the perforation is calculated as:

$$a_o = c'I \tag{5.9}$$

with 0.53 m $A^{-1} \leqslant c' \leqslant 0.79$ m A^{-1}. Equation (5.9) predicts that the size of the hole in the cover is roughly proportional to the current: for every 1 nA of current the hole has a radius between 0.5 and 0.8 nm (but noting that a_o increases discontinuously as the pit grows).

The shape factor in equation (5.7) was used to calculate the size of the hole in the pit cover for the transients of figure 2 (metastable pit growth) and figure 6 (stable pit growth). The results are shown in figures 12 and 13 respectively.

To calculate a_o in figure 13, a value of $\Delta C = 5$ M was used, since this corresponds

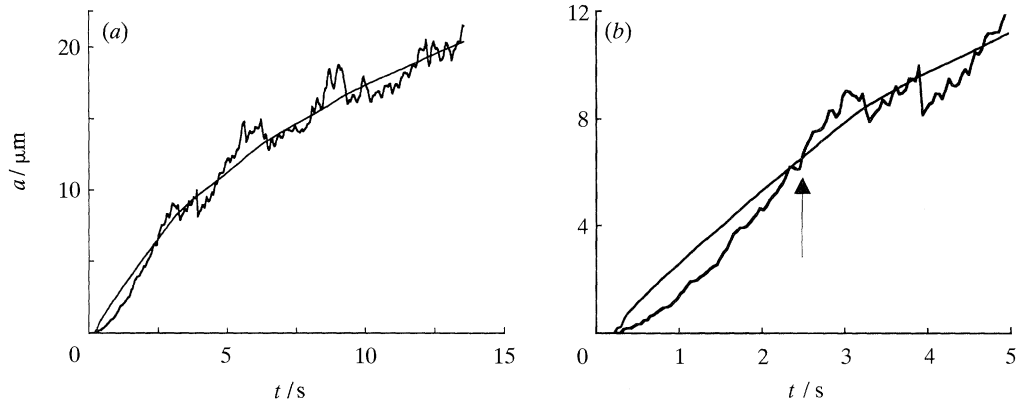

Figure 13. Calculated size of the hole in the cover over a pit which grows into a stable pit (data of figure 8). The smoother line is a_o; the noisier line is a_h. (*a*) The size of the hole in the cover is initially smaller than the pit radius (metastable growth). At $t = 2.5$ s, the calculated size of the opening in the cover becomes equal to the pit radius; beyond this point, the pit grows stably without a cover. (*b*) Expanded view of (*a*), showing the metastable growth stage more clearly.

to the average value of $ia = 0.5$ A m^{-1} during stable pit growth (figure 9). The basis of the link between the average ia value and ΔC is discussed further in §6*a*.

Figure 12 demonstrates how the pit radius increases roughly linearly with time while the pit grows metastably, and then reaches a plateau when the pit repassivates. As expressed by equation (5.9), the radius of the hole in the pit cover follows the current: the shape of the curve of a_o against t in figure 13 has the same form as the current transient itself (figure 3). This means that the mean hole radius, like the mean current increases on average in proportion to t^2. Because the pit radius is linear with t, the ratio a_o/a_h increases with t. The hole in the cover is largest, both in absolute terms and relative to the pit radius, just before repassivation. Figure 13 shows that the radius of the hole in the cover is then about one tenth of the radius of the pit.

The stably growing pit also requires a cover during the initial stage of pit growth. This is illustrated in figure 13, which shows that the calculated radius of the hole in the cover is smaller than the pit radius up to approximately $t = 2.5$ s. This is shown more clearly in figure 13*b*, in which the early time region of figure 13*a* is given in expanded form. Up to a time of 2.5 s a cover must be present over the pit mouth to sustain growth. After this time the calculated radius of the cover fluctuates noisily around the pit radius. This means that the pit is open: it is now deep enough to maintain the aggressive solution inside the pit without the necessity for any other barrier to diffusion. The observation is compared with figure 9, which indicates that the time of $t = 2.5$ s agrees approximately with the moment when the pit stability product (ia) reaches the constant value about which it too fluctuates at longer times. This is the moment when the behaviour of the pit changes from growth at constant i (metastable growth) to growth at constant ia (stable growth). The fundamental similarity between metastable growth and the initial growth of stable pits is emphasized by figures 12 and 13. Stable pits are originally metastable: only when they have grown sufficiently for a cover to be unnecessary for continued growth, do they become stable.

PHILOSOPHICAL TRANSACTIONS OF THE ROYAL SOCIETY A MATHEMATICAL, PHYSICAL & ENGINEERING SCIENCES

(*d*) *Experimental confirmation of diffusion control*

Implicit in the discussion above is the fact that metastable pits grow at a diffusion-controlled current density (which is constant with time). Frankel *et al.* (1987) have argued that the current density in metastable pits is under ohmic control, which means that the current density depends linearly on the potential. Because metastable pits growing at higher current densities are more likely to become stable (see §6*c*), ohmic control would offer a straightforward explanation for the potential dependence of stable pit formation. However, the present work indicates that the current in metastably growing pits is not under ohmic control, but is in fact diffusion-controlled. This conclusion is drawn from the results of polarization tests on single metastable pits, carried out as follows. The electrode was held at constant potential (0.7 V) until a single metastable pit had started to grow. During pit growth, the potential was swept in the negative direction at a rapid rate of 1 V s^{-1}. The entire current transient from the single pit was recorded, and the current density calculated from the recorded current. The results from one such a polarization experiment are shown in figure 14. Figure 14*a* shows the current transient from the metastable pit which started growing at 0.7 V and was then subject to the negative potential sweep. The time $t = 0$ is chosen to coincide with the start of the sweep from the initial holding potential of 0.7 V. It is seen that, until the onset of repassivation, the pit continues growing in the same manner after the potential sweep has started: the growth of the pit is apparently not affected by the change in potential. This is confirmed by figure 14*b*, which presents the calculated current density as a function of time, and figure 14*c*, in which the current density is plotted against the applied potential. Clearly, the current density in the growing pit is independent of the applied potential, over a range of *ca.* 300 mV. The deduced potential independence is valid, however, only if the remaining passive surface of the electrode surrounding the single pit contributes negligibly to the current transient. Figure 15 illustrates a current transient generated in a similar fashion to that shown in figure 14, but this time where the surface is fully passive. The diagram shows that the passive surface generates but a few nA under the negative potential sweep and its effect on figure 14 may be neglected. Figure 14 establishes then, that metastable pit growth is not under ohmic control of the current density, but under diffusion control.

Quantitative consideration of the ohmic potential drop in the electrolyte lends support to the suggestion that metastable pits grow under diffusion control (Pistorius & Burstein 1991). These calculations indicate that a salt film is present on the dissolving surface of the pit. The salt film forms because the concentration of metal cations (produced by anodic dissolution) reaches the saturation concentration of the chloride salt at the surface of the pit. The thickness of this film is by far the largest part of the ohmic potential drop (Hunkeler *et al.* 1987), and is 'self-regulating', in that it responds to potential changes to balance the current from the pit with the diffusional flux in solution (Isaacs 1973).

Stable pits, like metastably growing pits, are expected to grow under diffusion control, with the metal cation concentration at saturation at the inner surface. Equation (5.2) predicts that for diffusion control of stable pit growth, and putting $\Delta C = 4.2$ M (the solubility of $FeCl_2$ as determined by Kuo & Landolt (1975)), $ia = 0.42$ A m^{-1}. The experimental value of ia is a little larger than this, at 0.48 ± 0.03 A m^{-1} (figure 9). The discrepancy may be related to the fact that the pits are not quite hemispherical, but slightly dish-shaped (see §3). The size of this effect

Figure 14

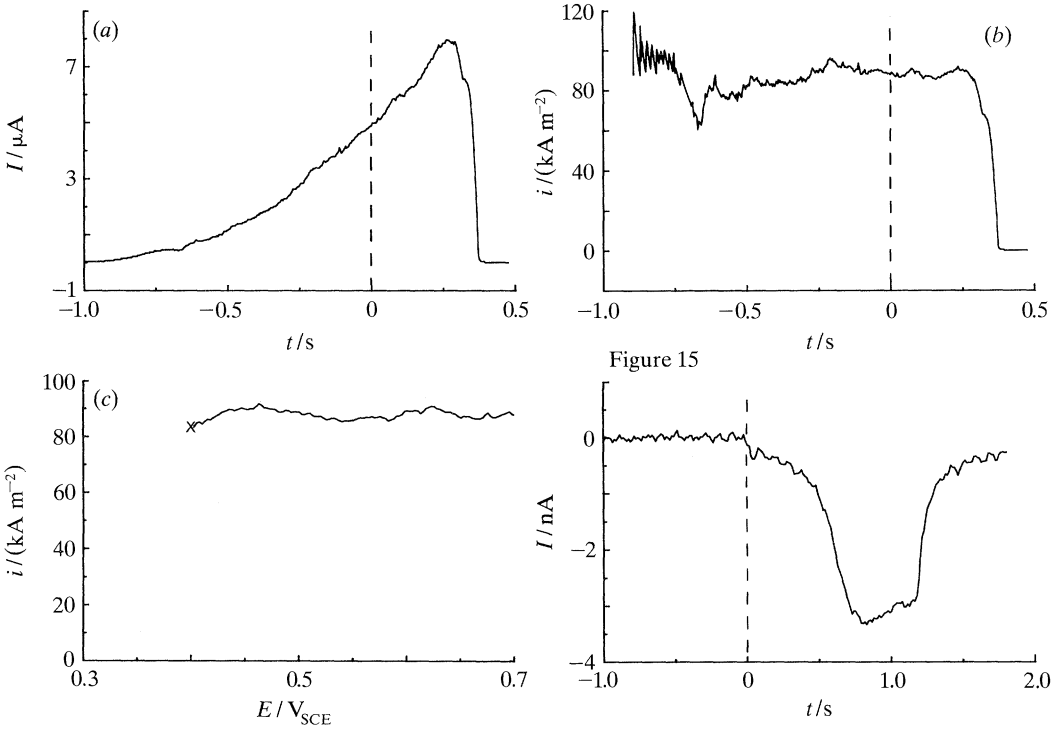

Figure 15

Figure 14. Results from a polarization test on a metastable pit. The metastable pit formed at 0.7 V, and was allowed to grow for about 1.0 s before a cathodic potential sweep at 1 V s^{-1} was applied. The cathodic sweep started at $t = 0$ s, indicated as a broken line. (*a*) Current transient. (*b*) Calculated current density in the pit, showing that pit growth is unaffected by the change in potential, up to the onset of repassivation. (*c*) Polarization curve, obtained by plotting the current density data for $t \geqslant 0$ s against the applied potential. The onset of repassivation is marked by a cross.

Figure 15. Cathodic current transient from the passive surface when no growing pit was present. The electrode was initially held at 0.7 V; a cathodic sweep at 1 V s^{-1} started from this potential at $t = 0$ s (indicated as a broken line), and stopped at −0.45 V, $t = 1.15$ s.

may be estimated from figures 3 and 5. The average $a_{\text{true}}/a_{\text{calc}}$ is 1.14 for the dish-shaped pits (see figure 3). For this ratio, the true area of the pit is 1.02 times as large as the calculated value (see figure 5), and the pit is 0.86 times as deep as the calculated radius. Thus the true value of ia is estimated to be 0.40 ± 0.03 A m^{-1}, in close agreement with the predicted value. This provides further evidence that the growth of pits, both metastable and stable, is under diffusion control.

The rest of this paper deals with the way in which the electrode potential affects the transition from metastability to stability.

6. The transition from metastable to stable growth

(*a*) *Effects of electrode potential on the metastable–stable transition*

It has been demonstrated above that the minimum pit stability product is not attained during metastable pit growth and the initial stage of stable pit growth, thereby requiring a flawed cover over the pit mouth to maintain propagation: the

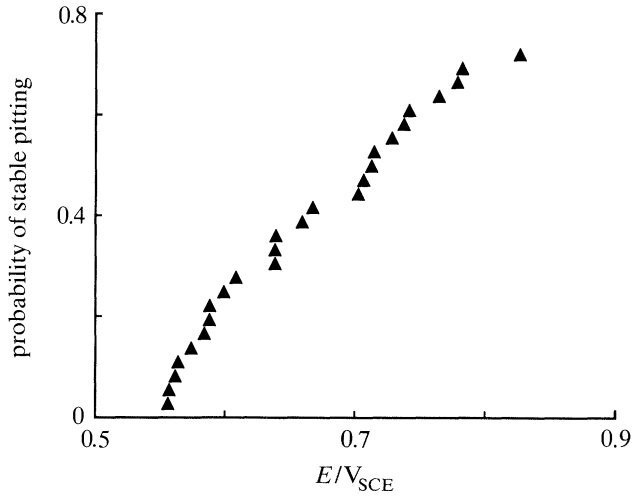

Figure 16. Potentials at which stable pits were observed during potentiodynamic testing at 2 mV s^{-1}, summarized as the probability of the formation of a stable pit.

transition from metastability to stability of the growth of the pit is linked to the properties of this cover. However, the transition to stability also depends on the electrode potential, as demonstrated by the existence of a pitting potential. The pitting potential is a probabilistic value which reflects the increasing probability of forming a stable pit as the potential becomes more positive, defined by a minimum probability (Shibata & Takeyama 1977).

The potential dependence of stable pit formation, as observed in the present work, is illustrated in figure 16. The results were obtained from 35 identical potentiodynamic sweeps from -0.45 V at 2 mV s^{-1}, each using a freshly ground electrode surface. The figure describes the probability of formation of a stable pit during the sweep as a function of the potential. The probability is calculated as $p(E) = n/(1+n_{tot})$, where n is the number of specimens out of a total of n_{tot}, on which stable pits have formed up to the potential E (Shibata & Takeyama 1977). The figure illustrates that no stable pits were observed below 0.55 V, and that about 25% of the specimens survived to 0.85 V without formation of a stable pit. The potentials at which stable pits were observed are spread fairly evenly between these limits. The value of 0.55 V is far above the pitting potential normally reported for type 304 stainless steel in solutions containing 1 M Cl^-; for example, Leckie & Uhlig (1966) measured a pitting potential of *ca.* 0 V in 1 M NaCl. The very high pitting potential of the 50 μm electrodes used in the present work may be the result of the strong refining effect of the wire-drawing process on malleable inclusions (such as sulphides) or other pit nucleation sites. The lack of any stable pit below 0.55 V contrasts the observation of metastable pits formed throughout the passive regime, down to -0.19 V.

Since the growth of pits is under diffusion control (§6), it appears that the only avenue for an effect of the potential on the metastable–stable transition is through the nucleation process. This can be considered in terms of the number of nucleation sites and the nature of those sites.

Figure 17

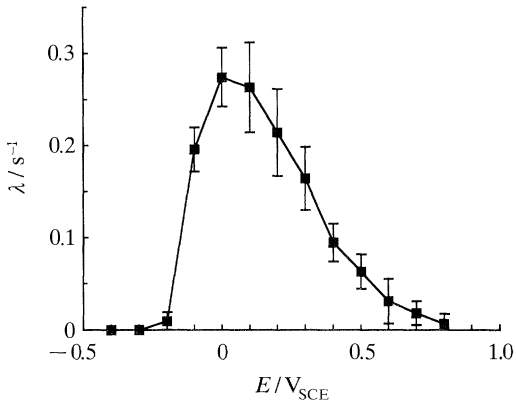

Figure 18

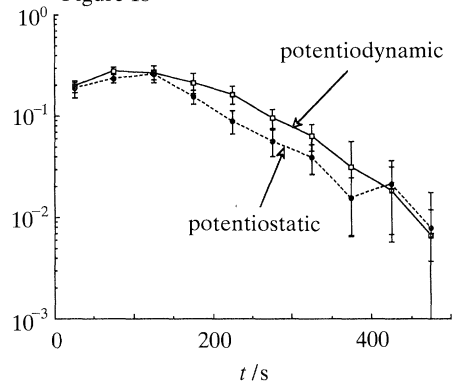

Figure 17. Rate of occurrence of metastable pits (λ) as a function of potential during potentiodynamic testing at 2 mV s^{-1}. Each data point gives the average for the surrounding 100 mV interval; scatter bars give the 95% confidence interval.

Figure 18. The decrease of λ with time under potentiodynamic conditions where the potential was swept at 2 mV s^{-1} (open points, solid line), and under potentiostatic conditions at $E = 0.1$ V (closed points, broken line). The diagram shows first order elimination of pit sites.

(*b*) *The rate of occurrence and the number of sites*

It is pertinent to consider the potential dependence of the rate of metastable pit occurrence and its possible link with the probability of forming a stable pit. Williams *et al.* (1985) expressed the link between the rate of formation of metastable pits (λ) and the rate at which stable pits form (Λ) as:

$$\Lambda = \lambda \exp(-\mu\tau_c), \tag{6.1}$$

where $\mu(s^{-1})$ is the probability of a metastable pit repassivating ('dying'), and $\tau_c(s)$ is a 'critical age': metastable pits which survive beyond τ_c were assumed to become stable. In terms of the discussion in §5, τ_c can be linked to the time taken to attain the critical pit stability product (*ia*) which is required for stable pit growth, and μ corresponds to the likelihood that the cover over the pit will rupture, causing the pit to repassivate before it can attain stability. If τ_c and μ are constants (independent of potential), equation (6.1) indicates that there is a simple correspondence between λ and Λ (Stewart & Williams 1990).

A plot of λ as a function of E is given in figure 17. The data were obtained from 50 identical potential sweeps, each on a freshly ground electrode surface, at 2 mV s^{-1} from a starting potential of −0.45 V. The number of metastable events was counted over 100 mV intervals (50 s period), and is plotted at the middle potential of each interval. The graph indicates that, above −0.2 V, the rate at which metastable pits occur increases rapidly to a maximum. At potentials greater than 0.1 V, λ decreases again. This unexpected decrease in λ at more anodic potentials apparently results from the elimination of pit nucleation sites from the surface of the electrode, rather than from changes in the passive film. It is shown in figure 18 that the elimination of sites follows first-order kinetics, allowing calculation of the potential dependence of the number of pit sites (N_o) which are present on the electrode surface before any pitting has taken place. Thus, if N is the number of pit sites available on the surface of the metal

$$\lambda = -\partial N/\partial t. \tag{6.2}$$

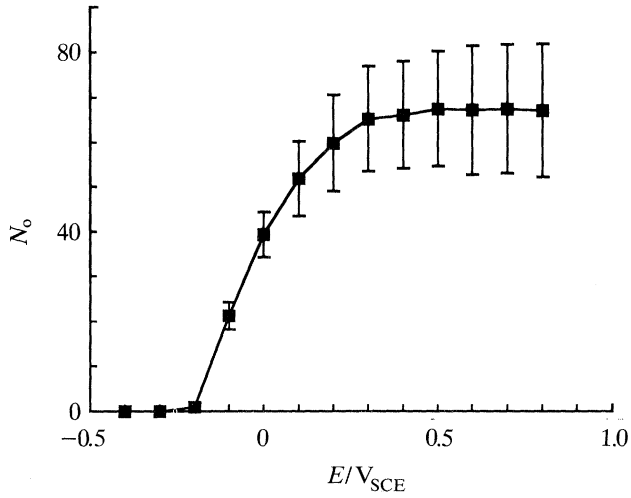

Figure 19. Dependence of the number of available pit sites on the electrochemical potential, as calculated from the data of figure 17.

First-order kinetics for site consumption implies

$$\lambda = N/\tau, \tag{6.3}$$

where τ is the first-order time constant. Combination of equations (6.2) and (6.3) and integration gives

$$N = N_0 \exp(-t/\tau). \tag{6.4}$$

Equation (6.4) is valid only under potentiostatic conditions. To evaluate the potential dependence of N_0 from a potentiodynamic sweep, N_0 is expressed as the sum of the number of sites present on the electrode (N) and the number of sites which have already been eliminated ($-\int dN$). Thus

$$N_0 = N - \int dN \tag{6.5}$$

and substituting equations (6.2) and (6.3) gives

$$N_0 = \lambda\tau + \int \lambda \, dt. \tag{6.6}$$

The results of this calculation are given in figure 19. It is immediately apparent that the pitting potential of 0.55 V (figure 16) is not associated with any particular increase in the number of sites. Indeed, figure 19 shows that N_0 is constant for potentials greater than 0.4 V. The transition from metastable to stable pitting is thus not linked to the number of sites. Likewise, no link between λ and the transition to stability is apparent: in the potential range where stable pits are observed (above 0.55 V), λ is relatively small (figure 17). Thus if the potential dependence does not lie in the number of nuclei, nor in the rate of nucleation, it must lie in the nature of the pit nuclei.

Any discussion of the nature of the pit nuclei is hampered by the lack of any direct experimental data. The available data refer to metastable pit growth, rather than the nucleation itself. If one adopts the pragmatic definition that the nucleation process is the process that leads to the formation of an experimentally observable pit, these data may provide clues to the nature of the nucleation process. The potential

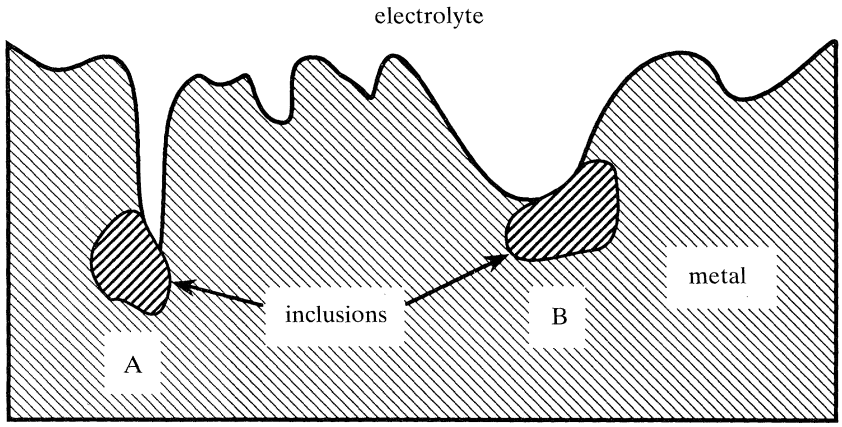

Figure 20. Suggested nature of a pit initiation site, which may account for the observed potential dependence of the number of pit sites. An electrochemically active inclusion is exposed at the base of a depression in the metal surface. Dissolution of the inclusion changes the local electrolyte composition, but this composition change is counteracted by diffusion. Since diffusion from site A is more restricted, this site can be activated at a lower potential than B.

dependence of N_0 (figure 19) indicates that nucleation is an electrochemical process. A second relevant observation is that the number of sites is strongly influenced by the surface roughness: if the roughness is greater, more pit sites exist (Morach & Böhni 1991). A higher chloride concentration also increases the number of sites (Stewart & Williams 1990; Pistorius 1991). A final observation concerns the rarity of pit sites. At high anodic potentials, there are *ca.* 70 sites present on the surface of the 50 μm electrode (see figure 19). The metastable pits which form on these sites grow to an average radius of *ca.* 1 μm before they repassivate. Thus when all the sites have been activated and repassivated, only some 10% of the surface is covered with pits; the combined area of the original sites from which these nucleated must be a significantly smaller fraction of the total electrode surface. The rarity of sites suggests that they must be of composition significantly different from the average composition of the alloy (Isaacs 1989).

Figure 20 illustrates one model of the pit site which is in accordance with the observations described above. In the figure, active sites are represented as electrochemically active inclusions at the bottom of depressions in the metal surface. These inclusions may be sulphides as has often been suggested (Szklarska-Smialowska 1986) or they may be simply large iron-rich clusters (Williams *et al.* 1991). Indeed, any electrochemically active site, which involves metal dissolution may be responsible for pit nucleation. The overall mechanism can then be envisaged: dissolution of metal cations causes migration of chlorides into the depression, creating an occluded cavity. In addition, dissolution of a sulphide inclusion may release thiosulphate ions, which accelerate dissolution of the metal (Lott & Alkire 1989). The dissolution rate is enhanced, consequent upon the higher chloride concentration, and hydrolysis of the metal cation enhances the local acidity. More rapid dissolution produces more rapid ingress of chloride, and dissolution then becomes self-sustaining. The activation of the site into a metastably growing pit constitutes the nucleation process. Following Galvele (1976, 1981) it is assumed that activation of the pit site requires a certain minimum product of the dissolution rate (current density) inside the pit site and the depth of the depression. The envisaged

Figure 21

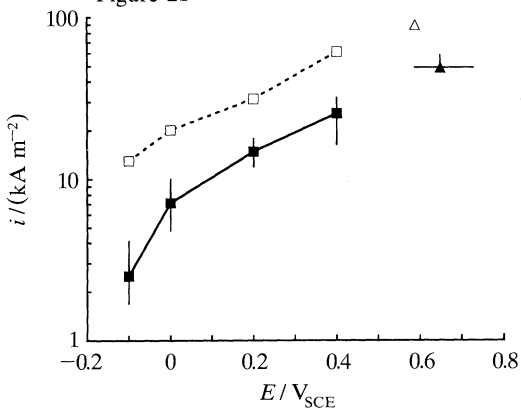

Figure 22

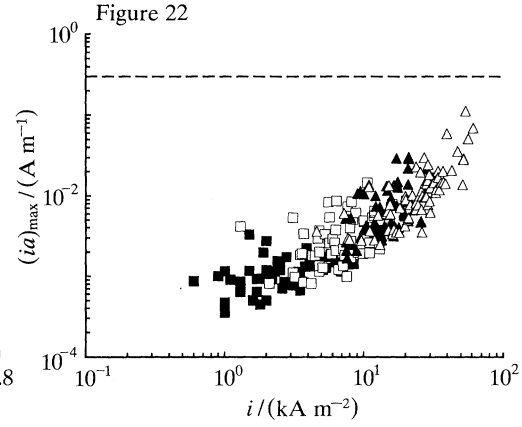

Figure 21. Current densities during metastable growth, for pits which repassivated (squares), and in pits which grew to become stable (triangles). Closed symbols give median values; scatter bars stretch from the lower quartile to the upper quartile. Open symbols give maxima. The metastable pit data were measured under potentiostatic conditions. The data from stable pits were measured under potentiodynamic scans at 2 mV s^{-1}.

Figure 22. Maximum value of the pit stability product achieved in each metastable pit, plotted against the current density in the pit. ■, −0.1 V; □, 0 V; ▲, 0.2 V; △, 0.4 V. The broken line is the minimum value of *ia* required for stability.

role of the potential in the nucleation process is to change the dissolution rate. The role of surface roughness is to act as a barrier to diffusion, providing a distribution of depressions in the metal surface. The chloride concentration may also influence the initial dissolution rate, either directly or through the magnitude of the ohmic potential drop in the solution within the depression. According to this model, the number of sites is larger at more positive potentials because the higher dissolution rate inside the pit site allows shallower, or more-open pit sites to be activated. Thus in figure 20, site B requires a higher current density, and thus a higher potential to activate than site A simply because it is shallower and wider.

(*c*) *The potential dependence of the nature of pit sites*

It is suggested above that the nature of pit sites changes as the electrode potential becomes more positive: at higher potentials, more-open sites can be activated. Some reflection of this change may be expected in the growth of pits which form at these sites. Data on the potential dependence of the growth rate of metastable pits are presented in figure 21. The growth rate is described by the current density which is approximately constant during metastable pit growth. These data were obtained from potentiostatic experiments at four holding potentials, with at least 50 transients analysed at each potential. Also shown on the graphs are the initial current densities from the metastable stage of 26 pits which grew to become stable: these were observed during potentiodynamic sweeps at 2 mV s^{-1}. Because the growth of these pits is very rapid and stability is attained within a few seconds (see figures 5, 7 and 8), there is only a very small change in potential (less than 10 mV in all cases) during the time interval over which these current densities were determined, and these data too, are regarded as potentiostatic. The data refer to the same stable pits for which the potential distribution is given in figure 16. In figure 21 the data points are the median values with the scatter bars stretching from the lower to the upper

PHILOSOPHICAL TRANSACTIONS OF THE ROYAL SOCIETY A MATHEMATICAL, PHYSICAL & ENGINEERING SCIENCES

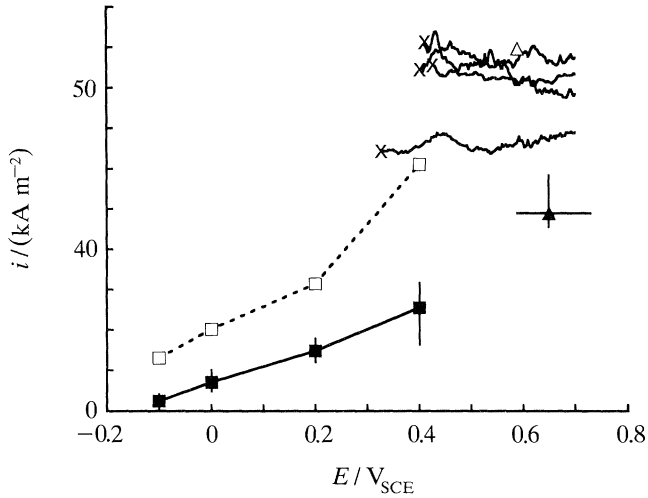

Figure 23. Potentiodynamic polarization curves of single metastable pits (formed at 0.7 V, then swept in the negative direction at 1 V s^{-1}), the end of which are marked with crosses, superimposed on the potentiostatic data of figure 20.

quartile. Figure 21 shows that the distribution of the pit current densities in metastably growing pits shifts to higher values at more anodic potentials. In addition, the pits which become stable generally grow at higher current densities than those which repassivate, although there is some overlap between the respective current distributions. The importance of the current density in the transition from metastability to stability is emphasized by figure 22. This figure plots the maximum pit stability product, $(ia)_{max}$ against the pit current density for the same metastably growing pits as those used to derive figure 21. The maximum pit stability product is given by the product of the current density and the final pit radius to which the pit grows before repassivating. Because the final pit radius does not depend strongly on the current density (Pistorius & Burstein 1991), $(ia)_{max}$ is roughly proportional to the current density. Thus metastable pits growing at higher current densities approach more closely the minimum ia product required for stability (0.3 A m^{-1}) before repassivating, and are therefore more likely to become stable. This observation is supported by the data in figure 21.

The role of the current density in the metastable–stable transition and the shift of the distribution of current densities in metastable pits to higher values at more positive potentials (figures 21 and 22) indicate how the electrode potential affects the transition to stability: at more positive potentials the current densities are higher, with a greater likelihood that a stable pit will form. This important effect of the electrode potential on the distribution of current densities contrasts the lack of an effect of the potential on the current density in a single metastably growing pit (see figure 14). The data from four single-pit polarization tests (including the one in figure 14) are given in figure 23, superimposed on the data of figure 21. Figure 23 embodies an apparent paradox: although metastable pits grow under diffusion control (with a current density which is independent of the electrode potential), the population of metastable pits shows a definite shift to higher current densities at more positive potentials. This paradox can be resolved by invoking the suggestions made in previous sections. During metastable pit growth the pit mouth is covered by a perforated film. Metastable pit growth is under diffusion control; at more anodic

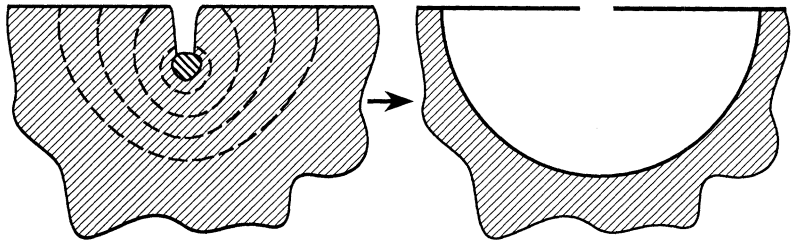

Figure 24. Conjectural mechanism by which the original degree of occlusion of the pit site may be reflected in the size of the perforation in the cover over the pit which grows from this site. The growth of the pit is shown as the succession of broken lines. The pit grows from an inclusion which is at the bottom of a depression in the metal surface. Once the pit starts growing, dissolution is more rapid closer to the mouth of the depression (whence diffusion is faster), than at the bottom; this eventually gives an approximately hemispherical pit. The pit cover is formed by the passive film, which is undermined by dissolution.

potentials more, and more-open sites can be activated into pits, as depicted in figure 20. This last point is a central one. Over the potential range to which figure 21 refers, the number of pit sites shows a strong increase (see figure 19). It is suggested then, that this increased number is linked to a change in the nature of the pit nucleation sites: specifically, as the potential is raised, more-open pit sites can be activated.

The diffusion-controlled current density in a metastable pit depends on the cation concentration at the surface of the pit, and the geometry of the pit. The concentration at the pit surface is the same at all potentials, since all pits grow in the salt-covered state (see §6*a*). Thus the only factor which can account for the effect of potential on the distribution of current densities is a potential-dependent change in the geometry of metastable pits. The pit geometry is described by the size of the pit, and the size of the perforation in the cover over the pit mouth. Since all pits grow to approximately the same size before repassivating (Pistorius & Burstein 1991), it is the nature of the pit cover which must be responsible for the potential dependence. Metastable pits which can only be nucleated at higher potentials must be more open, and must therefore have been nucleated at more-open sites. The implication is that there is a link between the geometry of the nucleation site and the hole in the cover over the pit which grows from that site: the form of figure 21 can be thus explained.

Because of the lack of direct information on the nature of the pit nucleation site, the nature of the link between the geometries of the site and the cover over the pit which grows from it can only be conjectured. One simple way in which this link may be made is shown schematically in figure 24. Dissolution is assumed to start from an inhomogeneity (similar to those shown in figure 20) which is at the bottom of a depression in the metal surface. Once dissolution starts, it is more rapid closer to the mouth of the pit, whence the diffusion distance is shorter, than at the bottom. As dissolution spreads, the passive film is undermined, and this film then forms the cover over the pit. The link between the geometry of the nucleation site and the hole in the cover over the resulting pit is then simply the width of the mouth of the original depression. A large perforation in the cover is expected over the metastable pit which grows from a more-open site and the pit consequently grows at a higher current density, but can only be activated at a higher potential. In a similar way, shallower depressions are expected to give larger perforations relative to the pit radius. These features describe the 'openness' of the nucleation site. The arguments suggest that the electrode potential affects the metastable–stable transition through

the nature of the pit sites which can be activated. At more anodic potentials, more-open pit sites can be activated; the metastable pits which grow from these sites are themselves more open and are thus more likely to grow into stable pits.

7. Conclusion

This paper focuses on the stability of the propagation of hemispherical corrosion pits on type 304 stainless steel in 1 M chloride solution. On the basis that a metal cation concentration of at least 3 M is required at the surface of a growing pit, it is predicted that open hemispherical pits can grow stably only if the product of the pit depth and the current density inside the pit, is larger than 0.3 A m^{-1}. This critical value of the pit stability product is not achieved in metastably growing pits, nor is it achieved during the early growth stage of pits which become stable. This implies that a perforated cover must be present over the mouths of metastably growing pits. Pit-growth stability is achieved only when the cover over the pit mouth is no longer necessary for its continued propagation. All experimentally observed pits, whether they repassivate or grow to achieve stability, initially grow metastably.

Metastable pits grow under diffusion control; the current density within a single pit is independent of potential. However, the distribution of current densities in different metastably growing pits shifts to higher values as the potential is made more anodic. Clearly, metastable pitting contains a potential-dependent step or steps (as is also indicated by the observation of a pitting potential), but this is not pit growth. It is proposed that pit nucleation is the potential-dependent step, a suggestion supported by the increase in the number of pit sites as the potential is made more anodic. This change with potential is thought to arise from the nature of the nucleation sites which can be activated through their geometry. As the potential is raised, more-open pit sites can be nucleated: these more-open sites grow into more-open metastable pits in which the current density is higher; it is shown that metastable pits growing at a higher current density are more likely to become stable.

Appendix A. Estimation of the shape factor for a concave hemisphere

Steady-state heat conduction, diffusion and ohmic current flow are all described by similar equations (respectively Fourier's law of heat conduction, Fick's first law of diffusion and Ohm's law). These equations for transfer of heat, mass or charge in the x direction are, respectively:

$$\text{heat conduction} \quad q_x = -kA_x \partial T/\partial x, \tag{A 1}$$

where q_x is the rate of heat transfer in the x direction, k is the thermal conductivity, A_x is the area of the conducting body perpendicular to the x direction and T is the temperature;

$$\text{diffusion} \quad (\partial m/\partial t)_x = -DA_x \partial C/\partial x, \tag{A 2}$$

where $(\partial m/\partial t)_x$ is the rate of mass transfer in direction x, D is the diffusion coefficient, A_x is the area perpendicular to x through which diffusion takes place and C is the concentration of the diffusing species;

$$\text{electrical conduction} \quad I_x = -\kappa A_x \partial \phi/\partial x, \tag{A 3}$$

where I_x is the current in the x direction, κ is the electrical conductivity, A_x is the

PHILOSOPHICAL TRANSACTIONS OF THE ROYAL SOCIETY A MATHEMATICAL, PHYSICAL & ENGINEERING SCIENCES

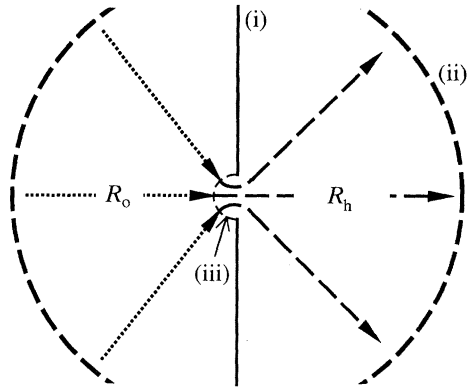

Figure 25. Configuration used to estimate the shape factor for an open hemisphere. Two infinitely large counter-electrodes are separated by a thin, planar insulating sheet which contains a circular hole with a radius a. (i) Thin insulating sheet containing a circular hole; (ii) counter electrode at infinity; (iii) imaginary hemispherical surface at opening in insulating sheet.

area perpendicular to x through which conduction occurs, and ϕ is the electrical potential. For heat conduction in multiple dimensions where only two temperature limits are involved, a conduction shape factor S may be defined (Holman 1986) so that

$$q = -kS\,\Delta T. \tag{A 4}$$

The shape factor has the dimension of length and describes the geometry of conduction. As such, the shape factor can be used to determine the current or diffusion rate for the geometry described by S, simply by replacing k and ΔT by κ and $\Delta\phi$, or by D and ΔC respectively. The estimate of shape factors below is for the electrical analogue.

(*a*) *Estimation of the shape factor for an open hemisphere*

The resistance between a circular disc of radius a, which is embedded in an insulating plane, and an infinitely large counter-electrode is equal to $1/(4\kappa a)$ (Newman 1966). Consider now two infinitely large counter-electrodes separated by a thin insulating sheet containing a circular opening of radius a (figure 25). From symmetry, the resistance between these two electrodes is approximately $1/(2\kappa a)$, i.e. twice that between a disc of this radius and one infinite electrode. The resistance between the two infinite electrodes is considered to be made up of two components: the resistance between one infinite electrode and an imaginary hemispherical surface at the opening in the sheet (R_o), and the resistance from this hemispherical surface to the second infinite electrode (R_h) (see figure 25). The former resistance is equal to $1/(2\pi\kappa a)$ (Holman 1986). Thus the resistance from the concave hemisphere to the counter-electrode at infinity is given by:

$$R_h = \frac{1}{2\kappa a} - \frac{1}{2\pi\kappa a} = \frac{1}{2\kappa a}\left(\frac{\pi-1}{\pi}\right). \tag{A 5}$$

From this, the shape factor for the open concave hemisphere is

$$S_h = 2\pi a/(\pi-1) = ca, \tag{A 6}$$

where c is a dimensionless constant which is predicted to be 2.934 for the concave

Table 1. *Measured resistances and shape factor constants for concave hemispherical electrodes and for a plane disc electrode*
(a, radius of electrode; R_{meas}, measured ohmic resistance; R_{∞}, resistance corrected for non-infinite counter electrode; $c = 1/(\kappa a R_{\infty})$ shape factor constant.)

electrode shape	a/mm	R_{meas}/Ω	R_{∞}/Ω	c
hemisphere	2.4	3139	3164	2.84
hemisphere	5.6	1207	1232	3.13
disc	5.6	924	949	4.06

hemisphere. The calculation is approximate because it assumes that there is no radial potential gradient across the opening in the insulating sheet of figure 25, and that the imaginary hemisphere is an equipotential surface.

The validity of the estimated value of c was tested by measuring the electrolyte resistance between each of two concave hemispherical electrodes (machined out of aluminium) and a large counter electrode. The radii of the hemispherical cavities were 2.4 mm and 5.6 mm. The resistance between a plane disc electrode (radius 5.6 mm) and the large counter-electrode was also measured. The counter-electrode was an aluminium foil lining on the inside of a plastic vessel measuring 0.22 m by 0.28 m wide by 0.15 m deep. The vessel was filled with tap-water of conductivity 46.3 mS m^{-1}. The hemispherical electrodes were placed at the water-line on the axis of the vessel. The electrolyte resistance was measured as the high-frequency limit of the a.c. impedance of the two-electrode cell, using a Solartron 1286 potentiostat and a Solartron 1250 frequency response analyser.

The results are presented in table 1. The table contains a correction for the finite size of the counter-electrode. This correction was estimated by calculating the resistance between a convex hemispherical electrode and infinity. This resistance, equal to $1/(2\pi\kappa a_{\mathrm{c}})$ (Holman 1986) is added to all measurements. The radius a_{c} is the radius of the circle having the same area as the cross-sectional area of the plastic vessel: this radius is 0.138 m, which yields a resistance of 25 Ω, and is a small fraction of the measured resistances (see table 1). The expected value of c for the plane disc electrode is 4 (Newman 1966): the measured value (4.06) is very close to this (table 1), providing some confidence in the validity of the measurements. The measured values of c for the hemispherical electrodes are close to the predicted value of 2.934. The shape factor for an open concave hemisphere is thus taken to be approximately $3a$.

(*b*) *Estimation of the shape factor for a covered hemisphere*

The arrangement considered here is that of a concave hemisphere of radius a_{h}, which is covered by a thin insulating sheet with a concentric circular hole of radius a_{o} (see figure 11). The resistance is again calculated by considering two resistances in series: the resistance between the inner surface of the hemisphere and a hypothetical isopotential hemisphere located at the opening in the cover (R_i in figure 26), and the resistance between this smaller hemisphere and infinity (R_{h} in figure 26). As in the previous section, R_{h} is estimated as

$$R_{\mathrm{h}} = (1/2\kappa a_{\mathrm{o}})\,(\pi - 1)/\pi. \tag{A 7}$$

R_i is given by (Holman 1986):

$$R_i = (2\pi\kappa)^{-1}\,(a_{\mathrm{o}}^{-1} - a_{\mathrm{h}}^{-1}). \tag{A 8}$$

Figure 26

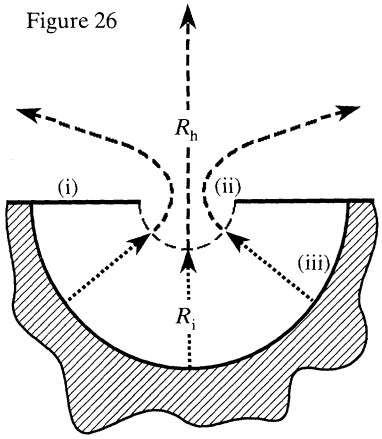

Figure 27

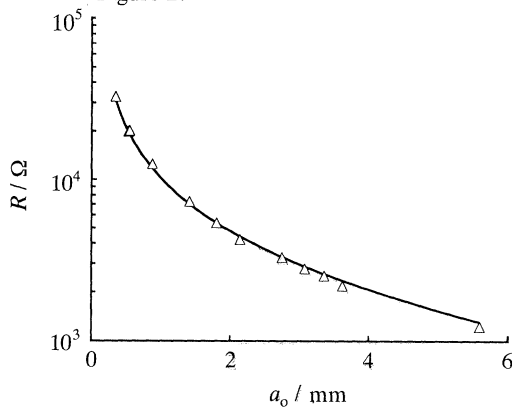

Figure 26. The resistance from the interior of the covered pit, to a counter-electrode at infinity, is assumed to be made up of two resistances: one inside the pit (R_i), and one from an imaginary hemispherical surface at the mouth of the pit, to infinity (R_h). (i) Cover over pit mouth; (ii) circular hole in pit cover of radius a_o; (iii) hemispherical pit of radius a_h.

Figure 27. Comparison between the measured (data points) and calculated (solid line) ohmic resistances between a concave hemispherical electrode (radius 5.6 mm) and a large counter-electrode, in a solution with a conductivity of 46.3 mS m^{-1}. The data are for a covered hemisphere, containing a single circular hole (radius a_o) in the cover.

The total resistance is then given by

$$R = (2\kappa)^{-1}(a_o^{-1} - (\pi a_h)^{-1}) \tag{A 9}$$

and the corresponding shape factor for the covered hemisphere is

$$S = 2a_o/(1 - a_o/\pi a_h). \tag{A 10}$$

The validity of this shape factor was again tested by measuring the ohmic resistance between a covered hemispherical electrode (radius of hemisphere 5.6 mm) and a large counter-electrode. The mouth of the hemispherical cavity was covered by a sheet of polyethylene (50 μm thick) which contained a single circular hole (the configuration of figure 11). A range of hole sizes was used. The measured and predicted values of the ohmic resistance are compared in figure 27, which shows that the correspondence is good.

References

Alkire, R. C. & Wong, K. P. 1988 The corrosion of single pits on stainless steel in acidic chloride solution. *Corros. Sci.* **28**, 411–421.

American Society for Testing and Materials 1989 ASTM annual book of standards, vol. 03.02, p. 1. Philadelphia: ASTM.

Brandes, E. A. (ed.) 1983 *Smithells metals reference book*, 6th edn, pp. 14–30. London: Butterworths.

Evans, U. R. 1951 Stress corrosion: its relation to other types of corrosion. *Corrosion* **7**, 238–244.

Ezuber, H., Betts, A. J. & Newman, R. C. 1989 Electrochemical kinetics in localized corrosion cavities. *Mater. Sci. Forum* **44**, **45**, 247–258.

Forchhammer, P. & Engell, H.-J. 1969 Untersuchungen über den Lochfraß an passiven austenitischen Chrom–Nickel–Stählen in neutralen Chloridlösungen. *Werkstoffe Korros.* **20**, 1–12.

Frankel, G. S., Stockert, L., Hunkeler, F. & Böhni, H. 1987 Metastable pitting of stainless steel. *Corrosion* **43**, 429–436.

Galvele, J. R. 1976 Transport processes and the mechanism of pitting of metals. *J. electrochem. Soc.* **123**, 464–474.

Galvele, J. R. 1981 Transport processes in passivity breakdown. II. Full hydrolysis of the metal ions. *Corros. Sci.* **21**, 551–579.

Gaudet, G. T., Mo, W. T., Hatton, T. A., Tester, J. W., Tilly, J., Isaacs, H. S. & Newman, R. C. 1986 Mass transfer and electrochemical kinetic interactions in localized pitting corrosion. *AIChE J.* **32**, 949–958.

Hakkarainen, T. 1990 Electrochemical conditions inside growing corrosion pits in stainless steel. In *Advances in localized corrosion* (ed. H. S. Isaacs, U. Bertocci, J. Kruger & S. Smialowska), pp. 277–282. Houston, Texas: National Association of Corrosion Engineers.

Holman, J. P. 1986 *Heat transfer*, 6th edn, pp. 77–82. Singapore: McGraw-Hill.

Hunkeler, F. & Böhni, H. 1987 Mass-transport-controlled pit growth on stainless steels and nickel. In *Corrosion chemistry within pits, crevices and cracks* (ed. A. Turnbull), pp. 27–42. London: Her Majesty's Stationery Office.

Hunkeler, F., Krolikowski, A. & Böhni, H. 1987 A study of the solid salt film on nickel and stainless steel. *Electrochim. Acta* **32**, 615–620.

Isaacs, H. S. 1973 The behaviour of resistive layers in the localized corrosion of stainless steel. *J. electrochem. Soc.* **120**, 1456–1462.

Isaacs, H. S. 1974 Potential scanning of stainless steel during pitting corrosion. In *Localized corrosion* (ed. B. F. Brown, J. Kruger & R. W. Staehle), pp. 158–167. Houston, Texas: National Association of Corrosion Engineers.

Isaacs, H. S. 1989 The localized breakdown and repair of passive surfaces during pitting. *Corros. Sci.* **29**, 313–323.

Isaacs, H. S. & Kissel, G. 1972 Surface preparation and pit propagation in stainless steels. *J. electrochem. Soc.* **119**, 1628–1632.

Kuo, H. C. & Landolt, D. 1975 Rotating disc electrode study of anodic dissolution of iron in concentrated chloride media. *Electrochim. Acta* **20**, 393–399.

Leckie, H. P. & Uhlig, H. H. 1966 Environmental factors affecting the critical potential for pitting in 18-8 stainless steel. *J. electrochem. Soc.* **113**, 1262–1267.

Li, W., Wang, X. & Nobe, K. 1990 Electrodissolution kinetics of iron in chloride solutions. VII. Experimental potential/current oscillations. *J. electrochem. Soc.* **137**, 1184–1188.

Lott, S. E. & Alkire, R. C. 1989 The role of inclusions on initiation of crevice corrosion of stainless steel. I. Experimental studies. *J. electrochem. Soc.* **136**, 973–979.

Mankowski, J. & Szklarska-Smialowska, Z. 1975 Studies on accumulation of chloride ions in pits growing during anodic polarization. *Corros. Sci.* **15**, 493–501.

Mankowski, J. & Szklarska-Smialowska, Z. 1977 The effect of specimen position on the shapes of corrosion pits on an austenitic stainless steel. *Corros. Sci.* **17**, 725–735.

Morach, R. & Böhni, H. 1991 Localized corrosion of high alloyed austenitic stainless steel. *Fourth international symposium on electrochemical methods in corrosion research*, Espoo, Finland. *Mater. Sci. Forum.* **111**, **112**, 493–505.

Newman, J. 1966 Resistance for flow of current to a disk. *J. electrochem. Soc.* **113**, 501–502.

Pistorius, P. C. 1991 Stability and metastability of corrosion pits on stainless steel. Ph.D. thesis, University of Cambridge.

Pistorius, P. C. & Burstein, G. T. 1991 Detailed investigation of current transients from metastable pitting events on stainless steel – the transition to stability. *Fourth international symposium on electrochemical methods in corrosion research*, Espoo, Finland. *Mater. Sci. Forum.* **111**, **112**, 429–452.

Riley, A. M., Wells, D. B. & Williams, D. E. 1991 Initiation events for pitting corrosion of stainless steel? *Corros. Sci.* **32**, 1307–1313.

Rosenfeld, I. L. & Danilov, I. S. 1967 Electrochemical aspects of pitting corrosion. *Corros. Sci.* **7**, 129–142.

Schwenk, W. 1964 Theory of stainless steel pitting. *Corrosion* **20**, 129t–137t.

Shibata, T. & Takeyama, T. 1977 Stochastic theory of pitting corrosion. *Corrosion* **33**, 243–251.

Stewart, J. & Williams, D. 1990 Studies of the initiation of pitting corrosion on stainless steels. In *Advances in localized corrosion* (ed. H. S. Isaacs, U. Bertocci, J. Kruger & S. Smialowska), pp. 131–136. Houston, Texas; National Association of Corrosion Engineers.

PHILOSOPHICAL TRANSACTIONS OF THE ROYAL SOCIETY A MATHEMATICAL, PHYSICAL & ENGINEERING SCIENCES

Stockert, L. 1988 Metastabile Lochfrasskorrosion. Dissertation ETH Nr. 8632, ETH Höngger-berg, Zürich, Switzerland.

Szklarska-Smialowska, Z. 1986 *Pitting corrosion of metals*. Houston, Texas: National Association of Corrosion Engineers.

Vetter, K. J. 1967 *Electrochemical kinetics: theoretical aspects*, p. 193. London: Academic Press.

Williams, D. E., Westcott, C. & Fleischmann, M. 1985 Stochastic models of pitting corrosion of stainless steels. I. Modeling of the initiation and growth of pits at constant potential. *J. electrochem. Soc.* **132**, 1796–1804.

Williams, D. E., Newman, R. C., Song, Q. & Kelly, R. G. 1991 Passivity breakdown and pitting corrosion of binary alloys. *Nature, Lond.* **350**, 216–219.

Received 29 November 1991; accepted 18 March 1992

PHILOSOPHICAL TRANSACTIONS OF THE ROYAL SOCIETY A MATHEMATICAL, PHYSICAL & ENGINEERING SCIENCES

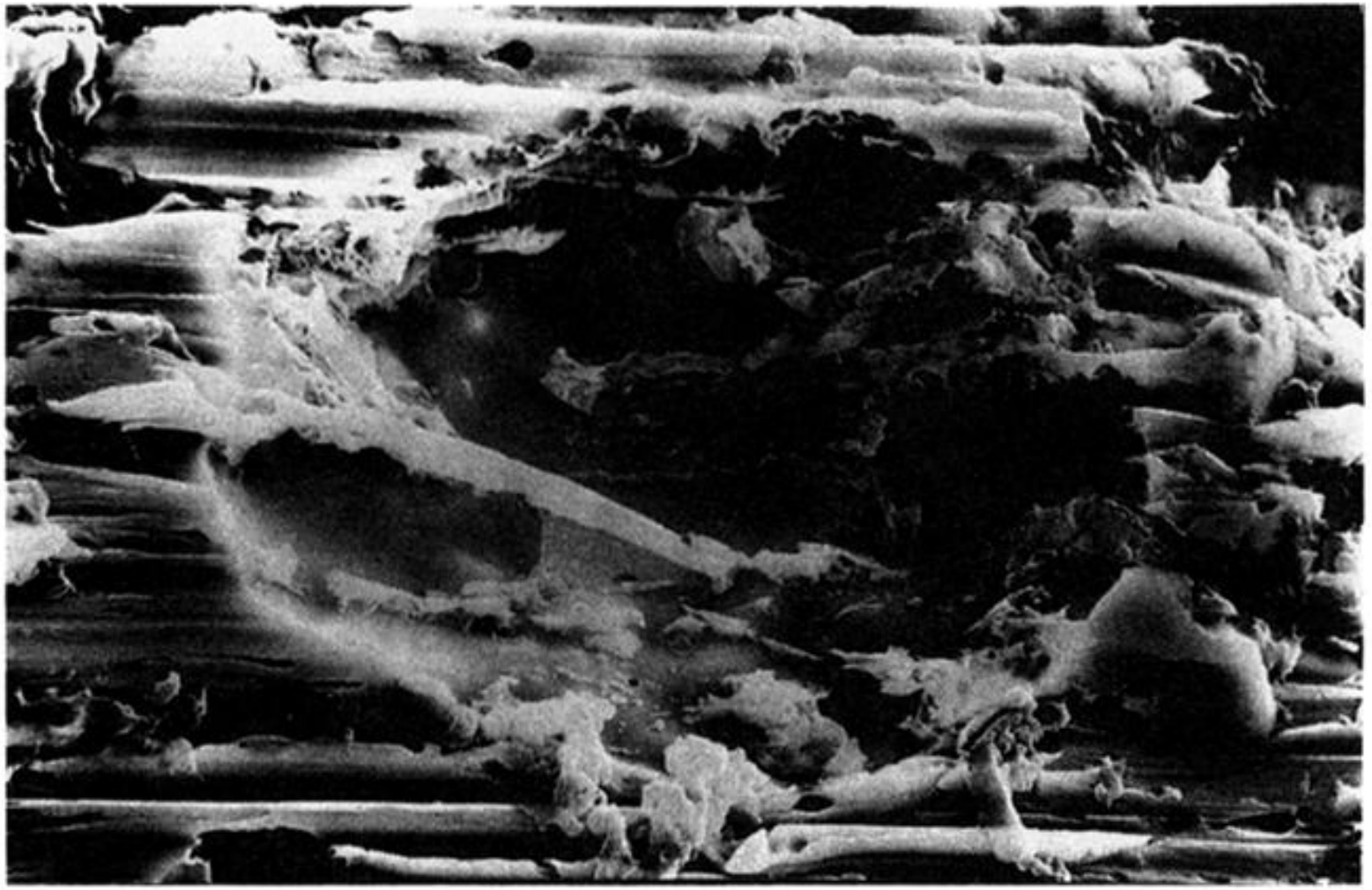

igure 10. Photomicrograph of a corrosion pit showing remnants of the cover over the pit mouth. he ligaments which extend into the pit interior are clearly part of what had been the original etal surface.